SANDIA REPORT

SAND2012-4433
Unlimited Release
May 2012

Graphene Resonators – Analysis and Film Transfer

Maria E. Suggs

Prepared by
Sandia National Laboratories
Albuquerque, New Mexico 87185 and Livermore, California 94550

Sandia National Laboratories is a multi-program laboratory managed and operated by Sandia Corporation, a wholly owned subsidiary of Lockheed Martin Corporation, for the U.S. Department of Energy's National Nuclear Security Administration under contract DE-AC04-94AL85000.

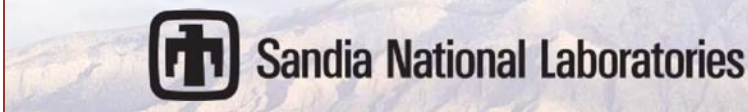

Issued by Sandia National Laboratories, operated for the United States Department of Energy by Sandia Corporation.

Available to DOE and DOE contractors from
U.S. Department of Energy
Office of Scientific and Technical Information
P.O. Box 62
Oak Ridge, TN 37831

Telephone: (865) 576-8401
Facsimile: (865) 576-5728
E-Mail: reports@adonis.osti.gov
Online ordering: http://www.osti.gov/bridge

Available to the public from
U.S. Department of Commerce
National Technical Information Service
5285 Port Royal Rd.
Springfield, VA 22161

Telephone: (800) 553-6847
Facsimile: (703) 605-6900
E-Mail: orders@ntis.fedworld.gov
Online order: http://www.ntis.gov/help/ordermethods.asp?loc=7-4-0#online

SAND2012-4433
Unlimited Release
Printed May 2012

Graphene Resonators – Analysis and Film Transfer

Maria E. Suggs
MEMS Technologies
Sandia National Laboratories
P.O. Box 5800
Albuquerque, New Mexico 87185-MS1080

Abstract

Graphene is a novel material with excellent material properties such as high elastic modulus, naturally one atomic layer in thickness, and highly conductive. Large area graphene can be grown on copper foils through chemical vapor deposition (CVD). The ultimate goal of this project is to fabricate and characterize suspended graphene resonators. In this work, we discuss the transfer of CVD-graphene (grown on a copper substrate) onto a dielectric-coated silicon substrate. We use equation of motion and finite element analysis to obtain eigenmodes of vibration of ideal graphene resonators.

ACKNOWLEDGMENTS

I would like to thank

Keith Ortiz for his support, encouragement and advice
Laura Biedermann for her daily support, guidance on the transfer process, and academic advice.
Mike Baker for the ANSYS tutorial
Paul Resnick for finding a suitable mask
Jose Luis Cruz-Campa for providing Si/Si_3N_4 chips for the transfer experiments
Everyone in 1719 and 1748 for their support

CONTENTS

FIGURES

1. INTRODUCTION

The simplest example of a resonator is a pendulum, executing simple harmonic motion. There exists a balance of forces, which trade energy throughout the cycle. A mass-spring system also resonates, with the balanced forces consisting of an inertial term and a spring (elastic) term. A resonator is so named because it is designed to operate at its resonant or natural frequency.

The resonator presented herein is a continuous or distributed system. This means that the mass and elasticity are not lumped into discrete masses and springs, but are treated as a continuously distributed material having mass and elasticity throughout its entire volume. The analysis strategy is generally to develop an equation of motion, using static analysis, considering all loads and boundary conditions, and then solve for the frequency of vibration. The finite-element method is also applied to solve for frequency, and is compared to the equation of motion analysis.

Graphene is the elastic material used for the construction of the resonator. Graphene is a two-dimensional material made from carbon, having a hexagonal lattice structure and a very strong C-C bond distance of 0.142 nm as shown in Figure 1[1],

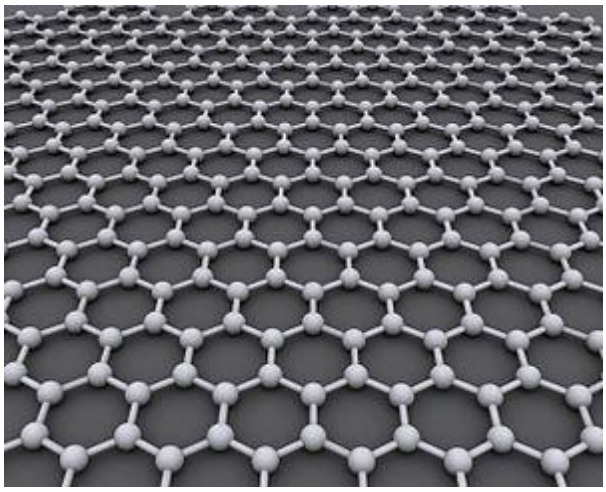

Figure 1: Graphene structure (after Wikipedia)

1.1. Background

In this work, two geometries of resonators are considered: beams and discs. The resonators are fabricated from Graphene, a carbon crystalline sheet that is only one atom in thickness. Graphene is usually obtained by exfoliation from graphite- a process that involves mechanically stripping loosely-adhered small single layer sheets of graphene from a block of graphite.[2] This process is adequate for basic research on graphene, but is not suitable for making useful resonators, as there are many problems with this technique. First, it is difficult to control where the flakes of graphene will land on the target substrate. Second, many of the flakes are not single-layer graphene. Third, the flakes are small, typically on the order of a few square microns.

This work presents a new transfer method for large area, single layer graphene using CVD growth of graphene on a copper substrate, followed by transfer to an oxidized and patterned silicon substrate. This method produces suspended sheets of graphene, suitable for use as resonators.

For any suspended structure, the details of the attachment of the suspended member to the substrate are important to the solution, and are known as the support (end) condition, or mathematically as the boundary conditions. The literature reports that the boundary conditions for transferred graphene in all geometries as a "clamped support" boundary. Mathematically, this is represented as,

Equation 1: The boundary conditions for a clamped structure

$$y(0) = 0 \qquad y(L) = 0$$
$$\frac{d}{dx}y(0) = 0 \quad \frac{d}{dx}y(L) = 0$$

Graphene is chosen as the resonator material for many of its special properties. Mainly, owing to the ultra-strong C-C bond, it has a Young's modulus of about 1 TPa, higher than most any known structural material. Secondly, it is naturally one atom in thickness, 0.335 nm. Additionally, the electron mobility can be extremely high, giving rise to excellent electrical conductivity even with such a thin layer. Graphene that has been transferred via exfoliation exhibits a strain in the 10^{-5} range, which is believed to be process-dependent. It is not yet known what strain will exist in the new CVD-transfer process.

1.2. Equations of Motion

Developing an Equation of Motion (EoM) for particular geometry, boundary conditions and loads involves first a static analysis of a differential segment of the resonator material, and a balancing of the forces. The specific solution to the resulting differential equation yields the resonant frequencies and the mode shapes.

1.3. Boundary Condition

The boundary conditions given above as Equation 1 are somewhat more complicated analytically than the case of a simply supported boundary condition, because it leads to a more complex mode shape that is not solvable in closed form. The first boundary condition dictates that the end is not allowed to move in the y-direction. The second boundary condition forces the beam to be horizontal at the end, relying on a bending moment to bend the beam away from the support, into the mode shape. These two boundary conditions are each applied twice to a beam, on each end- at $x=0$ and at $x=L$, for a total of four distinct boundary conditions. This is shown graphically in Figure 2.

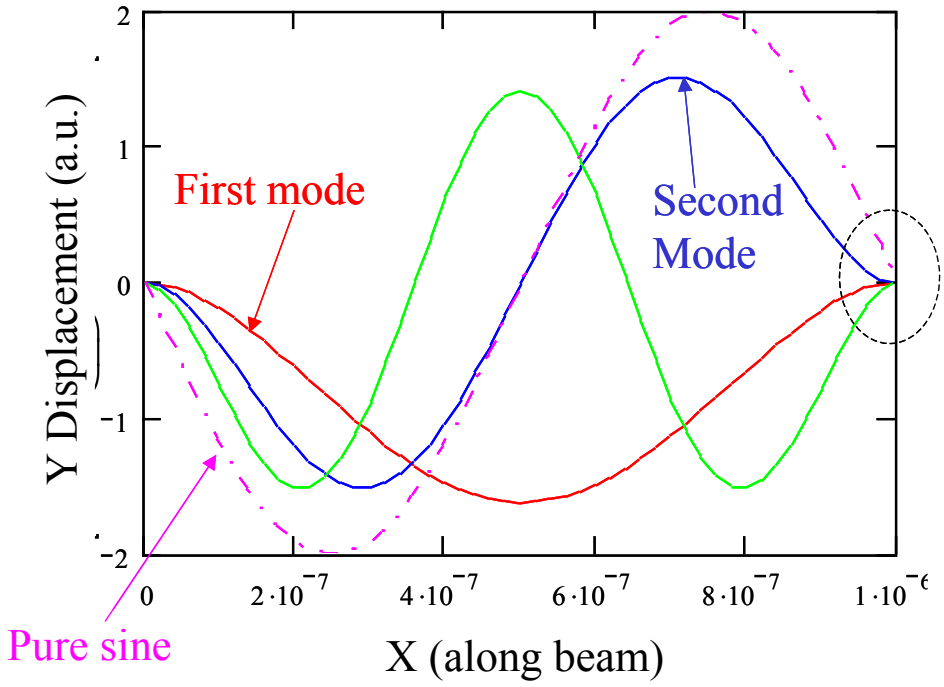

Figure 2: Three modes of a clamped beam, shown with a pure sinusoidal mode shape of a simply-supported beam for comparison.

The first three modes of a clamped (on both ends) beam are shown, along with a pure sinusoid. The "textbook" solution for vibration of a beam usually assumes a simply-supported boundary, because it leads to a sinusoidal mode shape, and a closed-form solution. The clamped boundary condition is mathematically unfortunate, because the solution involves combinations of hyperbolic trigonometric functions, which do not lead to the same closed form solutions, and require numerical solutions.

The clamped boundary condition ($\frac{dy}{dx} = 0$) can be observed in Figure 2, focusing on the right hand end. The pure sine wave is able to bend upwards immediately at the beam end- a necessary condition to achieve a pure sine wave. Comparing this to the second mode shape of the clamped beam, the beam remains horizontal for some distance from the end, only slowly curving upwards (under the bending stiffness constraint) to form the mode shape shown.

1.4. Loads

The loads are the *external* forces placed on the resonator. In the present case, there is one external load- the tension caused by the *intrinsic* stress, which results from the transfer process. In a later section, an *extrinsic* tension is applied by an electrostatic force, but the mathematical result is identical- The extrinsic tension simply adds algebraically to the intrinsic tension. Because this work presents a novel transfer process, the magnitude of the intrinsic stress is not yet known. Therefore, the analysis considers it. The literature-reported intrinsic strain for

exfoliated graphene is at least an order of magnitude higher than can be neglected, as is shown in the section below.

Axial loads in the plane of the sheet of graphene affect the resonant frequency. Because the graphene, as exfoliated, is under tensile strain, this load condition must be considered in the solution unless the strain for the new process is shown to be negligible. In the opposite extreme, a large tension could render the bending term negligible, simplifying the problem to a membrane analysis.

2. THE ROLE OF TENSION IN THE RESONANT FREQUENCY

There are potentially two restoring forces that balance the inertial force of the structure vibrating at resonance. Bending stiffness provides a restoring bending moment that acts to restore the structure toward equilibrium. Axial loads also act to restore equilibrium by minimizing the tension. In a simple analysis, it is desirable to identify one term as negligible and the other term as dominant to obtain a closed-form solution for the resonant frequency. However, one must determine which, if either, term can be neglected.

As an example, an approximate equation for fundamental resonant frequency (in Hz) of a beam including both tension and bending stiffness is,[3]

Equation 2: Approximate equation for resonant frequency of a clamped beam, including bending stiffness and tension

$$f = 1.03\sqrt{\frac{Et^2}{\rho L^4} + \frac{T}{3.4mL}}$$

Where E is Young's modulus, L is the length of the beam, m is the mass, T is the Tension, t is the thickness, and ρ is the density of the resonator material.

Numerous researchers report that exfoliated graphene is in tension, and that the amount of tension is dependent on the process used. They infer this by various experimental methods, but all methods arrive at the same conclusion: Exfoliated graphene is in tension, and the value of the strain is in the 10^{-5} to 10^{-4} range.

Bunch[4] states that graphene resonators exhibit a resonant frequency that is more than an order of magnitude (!) higher than simple plate theory would dictate, and attributes this difference to tension. Bunch further postulates that "The tension likely results from the fabrication process, where the friction between the graphite and the oxide surface during mechanical exfoliation stretches the graphene sheets across the trench." and quantifies the strain based on resonant frequency measurement as $2*10^{-5}$.

Chen[5] takes this a step further, dropping the bending stiffness term entirely, stating that "We use a continuum model that treats the graphene resonators as membranes with zero bending stiffness." Chen quantifies the strain in the 10^{-4} range, but this is complicated by what he terms "adsorbates" which increase the mass of the resonator. After an annealing process to remove adsorbates, the single-layer graphene strain decreases into the 10^{-5} range.

Frank[6] also measures the tension in a graphene film using force spectroscopy, indenting a suspended graphene sheet to obtain both Young's modulus and the tension in the film. Frank states, "In contrast to the fabrication of oscillators made from suspended carbon nanotubes that display significant slack, all the suspended graphene sheets made via exfoliation appear to be under tension." Frank states the average tension as 300nN in his structures, which span different thicknesses (not single layer).

Lee[7] also uses force spectroscopy, and quantifies the pre-strain as highly variable, with values ranging from mid 10^{-5} to mid 10^{-4}.

An important point for the above cited literature with regard to strain of suspended graphene structures is that these references all use mechanically exfoliated graphene. The literature also cautions that the strain is process dependent. The present project uses CVD-grown, transferred graphene, which may not exhibit the same strain after transfer. No measurement of strain from a similar process has been reported in the literature and this group has made no measurement, so the strain from this process remains unknown.

Given the strains reported in the literature, it is instructive to plot the resonant frequency using **Error! Reference source not found.** above to determine at what strain the tension term becomes dominant. Figure 3 shows frequency versus strain for two length beams, and assumes a clamped beam made of graphene using **Error! Reference source not found.**.

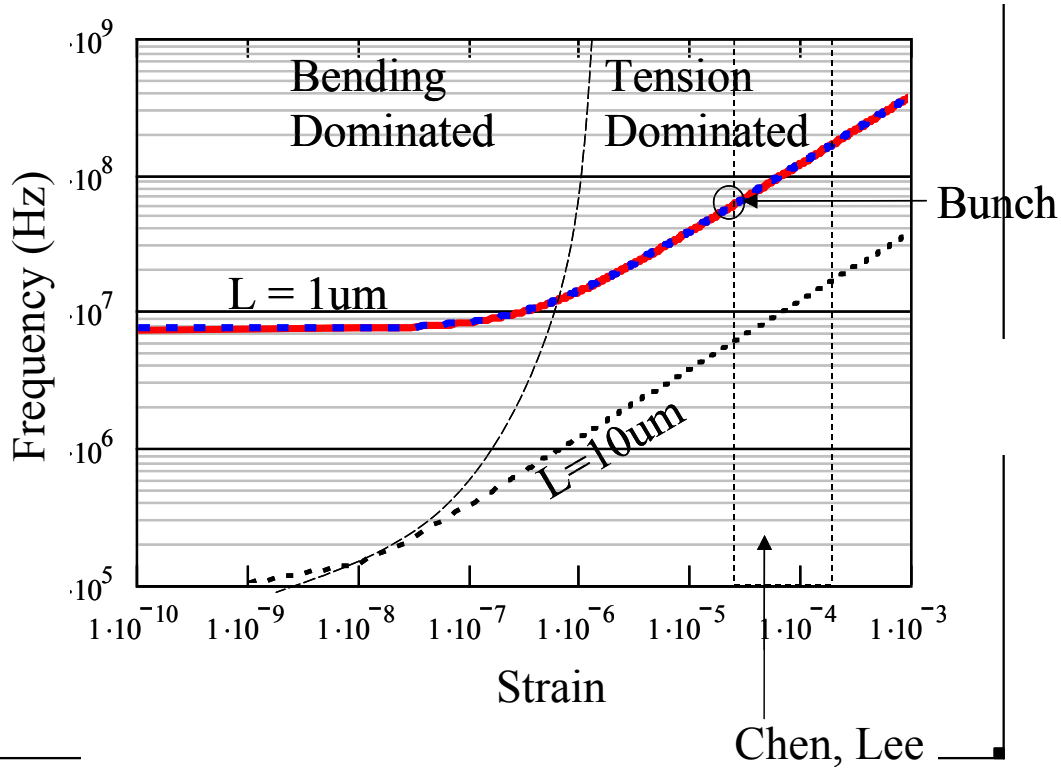

Figure 3: Regions of strain for which either bending or tension dominate the resonant frequency calculation of a graphene beam with clamped ends. Highlighted regions represent strains reported in the literature for exfoliated graphene.

Also note that this transition from bending-dominated to tension-dominated resonant frequency occurs at a higher strain for shorter beams, as can be seen by the L dependence in the equation, and in Figure 3.

2.1. Origin of the intrinsic strain

The literature is in agreement that the intrinsic strain is process dependent, and highly variable. It is postulated in Bunch's earlier work[4] that this may arise from friction during the exfoliation process.

Bunch[8] and Wong[9] both observe that the as-exfoliated graphene sheets tend to wrap down the sidewalls of the via over which it is suspended (Figure 4). Wong dismisses the possibility that this is caused by compressive strain in the graphene, as the graphene is observed to be in mechanical tension by static measurement. Bunch concludes the same, and further postulates that this results from the strong van der Waals interaction between the edge of the graphene membrane and the SiO_2 sidewalls, causing or further increasing the intrinsic tension. Hertel[10] provides a value for the energy of this attraction as 0.1 J/m^2, which gives rise to a tension of S = 0.1 N/m.[8] This tension would yield a strain in graphene of $\frac{S}{t \cdot E} \approx 10^{-4}$, which agrees with the resonance frequency derived strain obtained by Bunch[4] and the statics-derived strain of Chen, Frank, and Lee[5-7].

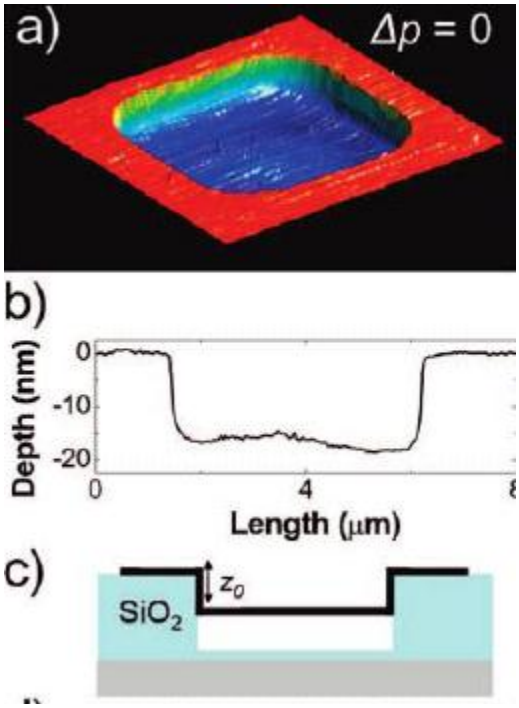

Figure 4: Graphene laminated onto silicon dioxide wraps down the sidewall of a via. After Bunch[8].

This observation may imply that the intrinsic tension is not entirely process derived, but may be inherent to the lamination of graphene over oxide vias. The variability in this tension appears to be process dependent, but some tension may be common to all lamination processes because of van der Waals forces between the graphene and the oxide substrate that cause the graphene to wrap down the sidewalls. This could be verified by fabricating a via made from an undercut, or reentrant sidewall profile.

2.2 Beam

The equation of motion for a beam under tension is[3]

Equation 2: Equation of Motion for a Beam, including tension and bending stiffness

$$E \cdot I \frac{d^4}{dx^4} y(x,t) - T \frac{d^2}{dx^2} y(x,t) = -\rho A \frac{d^2}{dt^2} y(x,t)$$

Equation 2 is derived by a static analysis of the forces on a differential element of the beam. The terms represent the bending moment, the axial tension and the inertia, respectively. The general form of the solution to this equation is given by[11]

Equation 3: General solution to the beam equation

$$Y = C_1 \sinh(\lambda_1 x) + C_2 \cosh(\lambda_1 x) + C_3 \sin(\lambda_2 x) + C_4 \cos(\lambda_2 x)$$

After application of the clamped boundary condition, all four terms remain in Equation 3, and the characteristic equation is solved numerically to find the resonant frequency. **Error! Reference source not found.** shows the frequency response for the first (fundamental) mode of vibration of a clamped beam analyzed with this method for variable length and intrinsic strain

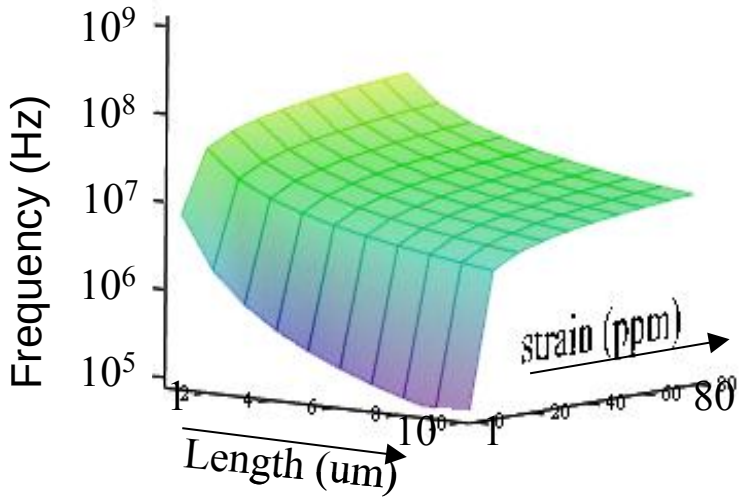

Figure 5: Frequency response surface for a clamped graphene beam, versus length of the beam and intrinsic strain in the resonator film.

The frequency response illustrates that the resonant frequency is higher for shorter beams, and for higher strain, as expected. Depending on which root of the characteristic equation is selected, a distinct mode of vibration is obtained (The first three of which are illustrated in Figure 2). **Error! Reference source not found.** illustrates the effect of mode number on the resonant frequency:

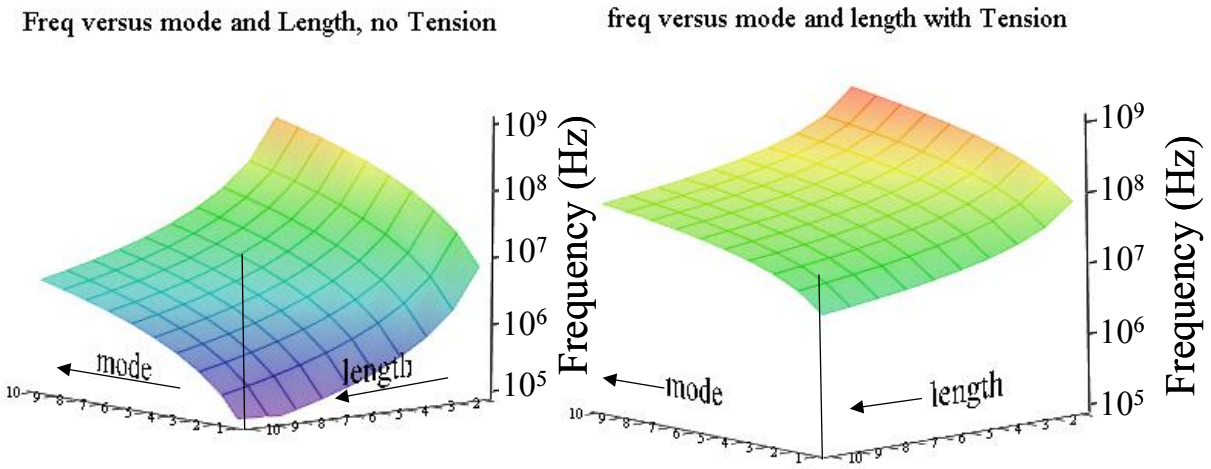

Figure 6: Frequency response for a clamped graphene beam versus length of beam and mode of vibration, for two different strain conditions.

From these figures, it is apparent that intrinsic tension has the effect of increasing the resonant frequency, but lessening the variation in resonant frequency with length, and modes. In the figure on the left, there is a four order of magnitude change in resonant frequency across a 10X change in length, and 10 modes. On the figure on the right, the same change in L and modes produces only a two order of magnitude change in resonant frequency. The implication of this is that there is less tunability at higher strain.

2.3 Disc

The equation of motion for a disc is given by[3]

Equation 4: Equation of motion for a disc, including tension and bending

$$\nabla^4(y) - \frac{T}{D}\nabla^2(y) + \frac{\rho}{D}\frac{d^2}{dt^2}(y) = 0$$

where T is the tension, ρ is the density of the resonator material, D is the flexural rigidity, and ∇ is the Laplace operator in cylindrical coordinates. This equation has a solution of the form[11]

Equation 5: General solution of the equation of motion for a disc with tension

$$y(r,\theta) = \left[C_1 J_n\left(\lambda_1 \frac{r}{a}\right) + C_2 J_n\left(\lambda_2 \frac{r}{a}\right)\right] \cdot \cos(n\theta)$$

where a is the disc radius, C_1 and C_2 are constants, J and I are solutions to Bessel's Equation, and Modified Bessel Equation, respectively, of order n. After application of the clamped boundary condition, the characteristic equation is solved to find the resonant frequency. Care must be taken

to obtain the correct corresponding modes, which depend on the Bessel order and the particular root of the equation.

Shown in Figure 7 is a mode shape calculated from the equation of motion for a disc with tension and a clamped boundary. The inset shows a cross-section of the mode shape from the disc-center to the right edge (red line). This mode includes one circular mode (in addition to the boundary) and one radial mode (into/out of the page). This mode is often referred to as *mode 1-2*, counting the first radial mode and the second (including the fundamental) circular mode. In this work, this is referred to as *mode 6* because in order of increasing frequency, this mode occurs sixth. If the tension is negligible, this mode would have a resonant frequency 5.98 times the fundamental. If tension is dominant, the resonance would occur at 2.92 times the fundamental frequency. With both terms included, the resonant frequency is between these two factors. The clamped boundary condition ($\frac{dy}{dr}$=0) is apparent at the right edge, similar to the beam mode shape near the clamped boundary.

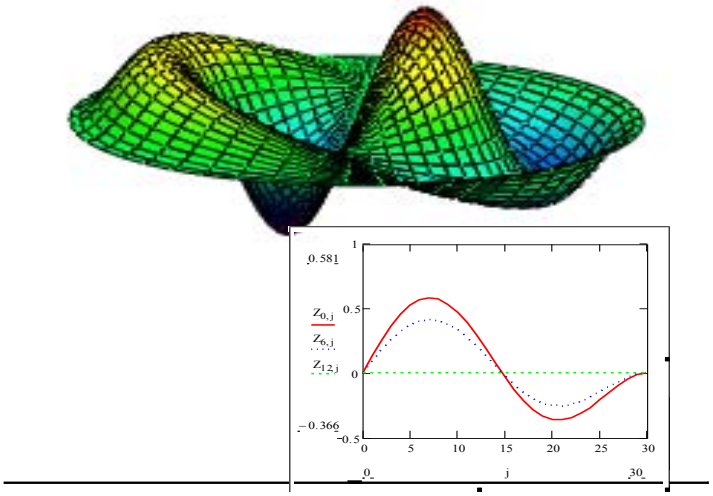

Figure 7: Mode shape of a clamped disc in the sixth mode of vibration (one radial mode and two circular modes, including the fundamental). The inset shows a cross-section from the disc-center to the right edge (red line).

After finding the roots and solving for the eigenvalues of Equation 5, the frequency response versus disc radius, film strain, and mode number can be obtained, and is plotted in Figure 8 for the first mode.

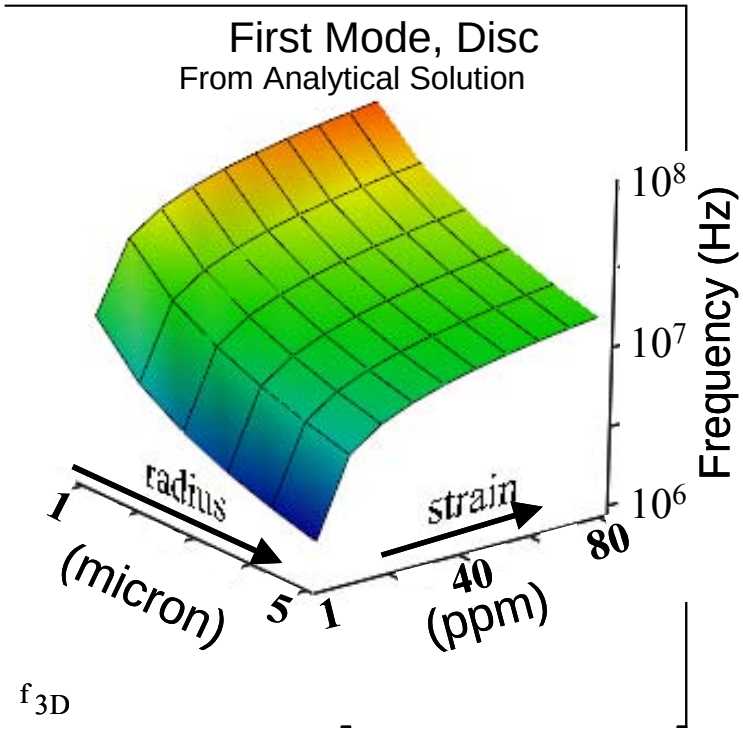

Figure 8: Frequency response surface for a graphene disc versus radius of the disc and strain for the fundamental mode.

Illustrating the mode is more complicated for discs, because there are two orthogonal modes: radial and circumferential. In this work, the modes for a disc are simply ordered by integer in order of increasing resonant frequency. This is, however, a mixture of radial, circumferential and radial-circumferential mixed modes. The mode shapes are illustrated in the finite element analysis (FEA) section below.

2.4 Finite Element Analysis

The finite element method is well suited for modeling structures such as the ones in this work. In this section, only the disc modeling using ANSYS is presented, and compared to the results from the Equation of Motion analysis. The structural element used for modeling the resonator is the ANSYS SHELL181, which allows for the input of material intrinsic strain.

The nine lowest resonant mode shapes are illustrated in contour plots in Figure 9, with the fundamental mode at the upper left, then progressing to the second mode (a radial mode) in the top center, the third mode (another radial mode) in the upper right, followed by the fourth mode center-left (a purely circular mode), and so on. The sixth mode, center-right, corresponds to the 3-dimensional mode shape illustrated in the previous section. One word of caution about contour mode shapes as in Figure 9, the phase of the various segments is not represented. This is apparent when comparing mode 6 from Figure 9, and the same mode represented in 3-dimensions from Figure 7.

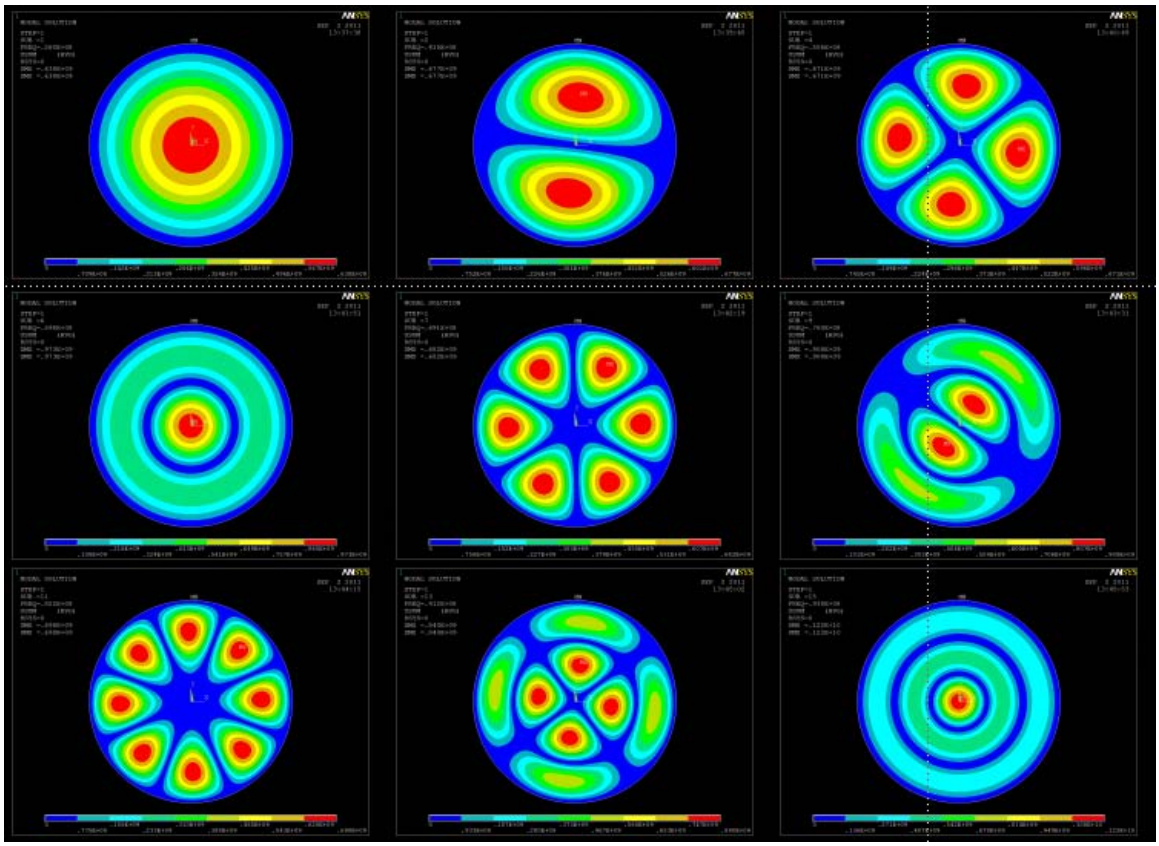

Figure 9: The first nine mode shapes of a clamped disc, obtained using ANSYS. Frequency increases left to right, and top to bottom. Corresponding resonant frequency values are shown in Figure 10.

The resonant frequencies corresponding to the nine modes represented in Figure 9 are shown in Figure 10, both in the case of no tension, and with a strain of 4×10^{-5}. These results are for a 2 micron radius (4 micron diameter) disc made of single layer graphene. The intrinsic strain causes a resonant frequency that is about an order of magnitude higher than the frequency of a structure having no intrinsic stress (bending only solution).

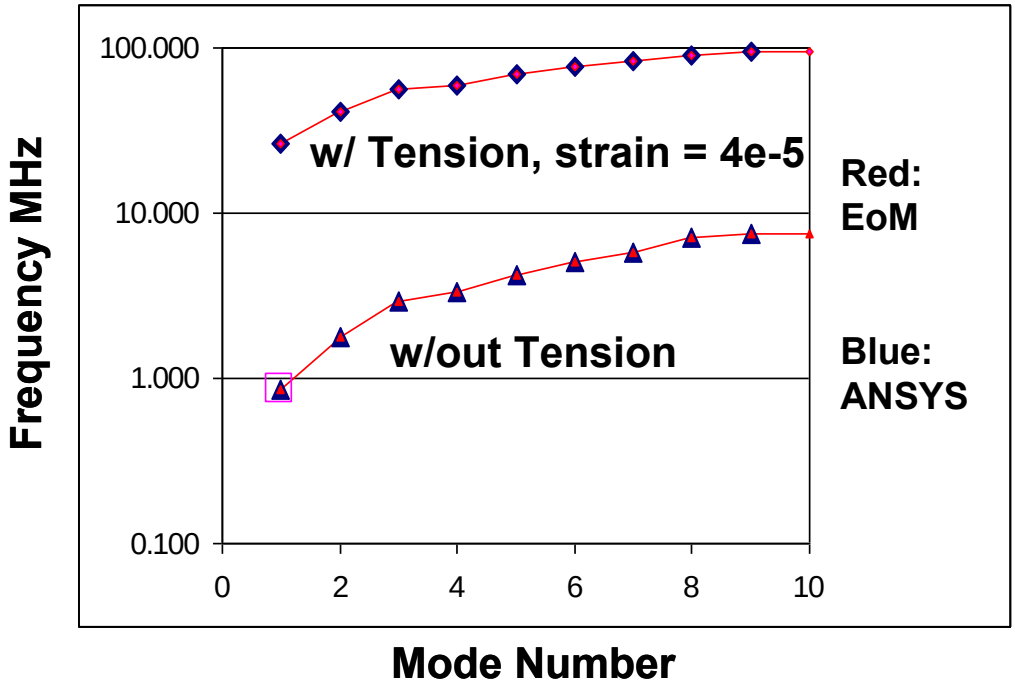

Figure 10: Resonant frequency of a graphene disc in different modes of vibration (as illustrated in the previous figure), with and without intrinsic strain. The disc has a radius of 2 μm. Blue triangles are obtained using ANSYS, and red lines are obtained from the equation of motion analysis.

Also shown on Figure 10 are the results from the Equation of Motion analysis. The ANSYS results are shown as blue triangles, whereas the EOM results are shown in red, connected by a line. The results from these two methods agree perfectly.

2.5 Exciting/Driving the resonator

Two things are needed to measure the action of the resonator. First, the resonator must be excited into resonance. Second, a measurement must be made to observe the oscillations.

In order to excite the resonator into vibratory motion, an external perturbation is required. At room temperature, thermal energy can excite a very small vibration in the structure, but this is difficult to detect. Two common methods of excitation are thermal and electrical.[12]

The easiest method to observe resonance in the laboratory is with thermal excitation. A laser is focused on the resonator, and pulsed near the resonant frequency, alternately heating and cooling the resonator. A separate laser having a different wavelength is used to make an interferometric measurement of the vibration.

Electrical excitation is more useful outside of the laboratory, as a simple circuit can be used to excite the resonator through electrostatic actuation, but this requires electrodes to be

integrated with the resonator. The motion of the resonator can also be detected electrically through a capacitance measurement.

2.6 Electrostatic tuning and tensioning

Because the resonant frequency is sensitive to in-plane tension, additional extrinsic tension above the intrinsic value, can be applied externally to tune the resonator's frequency to a desired higher value. The effect of externally applied tension on the equation of motion is exactly the same as the intrinsic tension, so no new terms need be added. The simplest approach to increase the tension in the suspended film is to electrostatically pull the film down toward the substrate by applying a "gate" voltage.[5] Chen reports that this voltage causes the resonant frequency of a beam to change as $\sim V_g^{2/3}$.

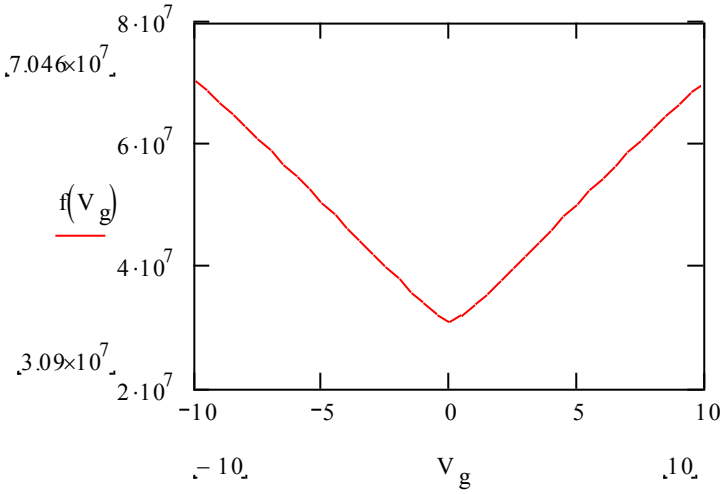

Figure 11: The role of a gate voltage in increasing the resonant frequency by tensioning the structure.

3. TRANSFER OF CVD-GROWN GRAPHENE

3.1 Transfer method

The process illustrated in Figure 12 is described sequentially as follows:

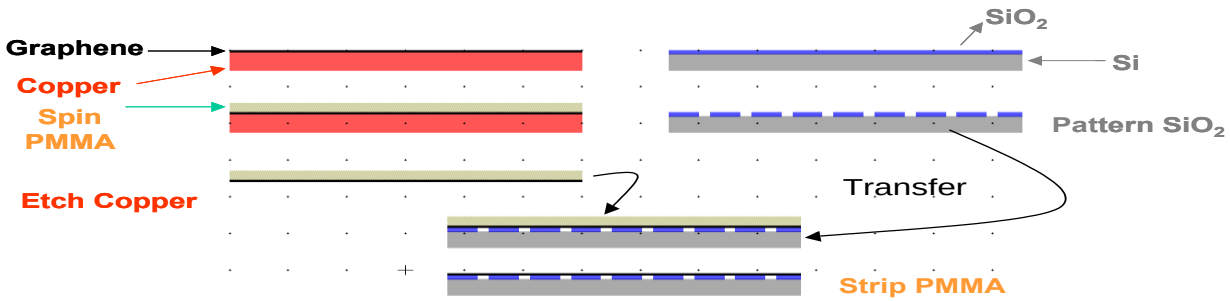

Figure 12: Wet process flow for transferring CVD graphene from copper to silicon

1) A monolayer of graphene is grown on a 20 μm thick film of copper (purchased from "Graphene Supermarket"), and cut into ~cm squares.
2) Spin 100 nm layer of PMMA (20 mg/mL), and place the PMMA/Graphene/Copper in a vacuum desiccator for three to five days to allow the PMMA to cure.
3) Place the PMMA/Graphene/Copper into copper etchant for approximately two hours. (Iron nitrate or ammonium persulfate).
4) After the copper has etched, flush the etching solution with DI water.
5) In parallel with steps 1-4, 100 nm of silicon dioxide is grown on a silicon substrate
6) Pattern and etch the oxide with vias and trenches of different sizes to form transfer receiver chip.
7) A wedge-shaped chip holder support, angled at 30 degrees, is placed inside the rinse water where the PMMA/Graphene is floating.
8) A pipette is used to pin the PMMA/Graphene on to the chip, and the water is drained.
9) As the water is drained, the PMMA/Graphene begins to adhere to the chip.
10) The chip is placed into the desiccator for at least one day to evaporate the remaining water.
11) Strip the PMMA from the graphene using one of the following methods.

a) solvents (acetone, methanol, isopropanol)
b) heated solvents
c) chlorobenzene and solvents
d) furnace anneal in air or in forming gas (H_2-N_2)

3.2 Problems with this method

1) There is difficulty in completely removing the PMMA after transfer without damaging the graphene.
2) Water is trapped between the graphene and the silicon substrate after wet transfer, because graphene is highly impenetrable.[8]
3) The PMMA layer, being ~1000 times thicker than the graphene, imparts stress to the graphene, causing cracks, wrinkles, and non-planar films.
4) This method seems not scalable to large (wafer) scale.
5) Cutting/shearing of the copper/graphene foil causes a very wavy, non-planar sample.

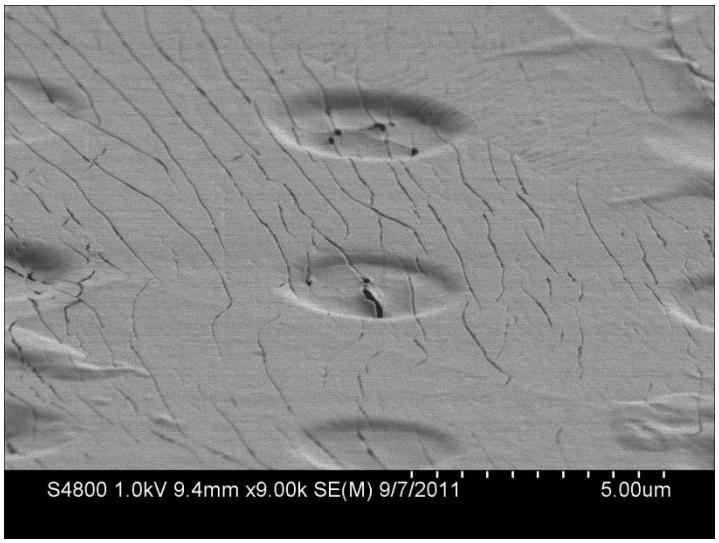

Figure 13: SEM Image of a PMMA/graphene transfer onto Si/SiO_2.

3.3 Improved transfer process

A new process is proposed.[13] The new process:

1) Is polymer free, which solves problem #1 and #3 in the previous section.
2) Is dry (on the substrate side), solving problem #2.
3) Is scalable, solving problem #4.
4) Applies pressure to the membrane as the copper is removed, keeping the graphene in intimate contact with the substrate during the copper removal.

To solve Problem #5, the copper/graphene foil can be cut via die ("cookie cutter") instead of shearing with scissors.

A schematic of the proposed apparatus is shown in Figure 14.

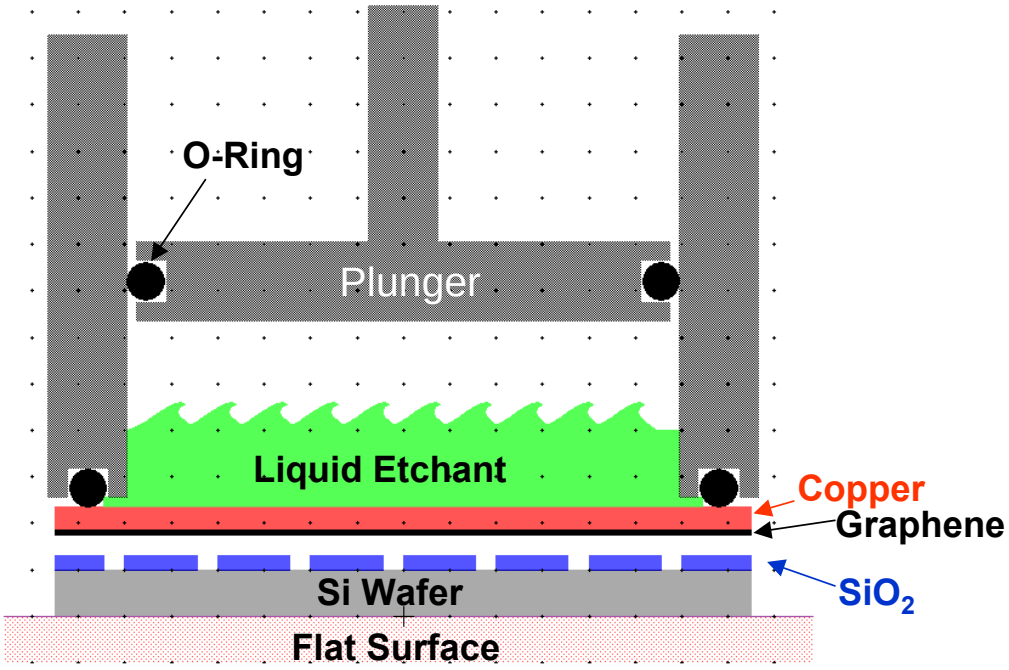

Figure 14: Proposed dry (Si wafer side) transfer process to solve many issues in the current wet process.

3.4 Intrinsic tension measurement

Several sources report force spectroscopy results on suspended graphene.[6-7] This method provides a direct measurement of the Young's modulus and intrinsic in-plane stress in the suspended film. An indentation is made using a standard AFM tip in order to deflect the membrane near its center. The force is measured by the deflection of the AFM cantilever of known stiffness. The deflection distance is measured by the movement of the AFM piezoelectric actuator, providing a force-distance curve.[14] A Least-squares fit of the measured data to Equation 7 below provides both the Young's modulus and the intrinsic in-plane stress

Equation 6: Force versus displacement relationship for a point-load indentation of a disc structure, used to obtain strain and Young's modulus.

$$F = \sigma_0 \pi \delta + Eq\frac{\delta^3}{a^2}$$

where F is the force, δ is the membrane deflection distance, σ_0 is the intrinsic strain, E is young's modulus, q is a constant and a is the resonator/disc radius.

Such an experiment for the new process described in this work should be conducted in order to obtain these parameters. This information can then be used to calibrate the resonant

frequency of the resonator structures and correlate the tension from this static measurement to that obtained via resonant frequency measurements.

3.5 Device design

A layout for the resonator Si substrate is generated with beams and discs in the range of 1-10 μm (length, or radius, respectively), to ensure that the resonant frequency of the structure is in the 10-15 MHz range, allowing a large range of strain in the new process. A snapshot of the layout is shown in Figure 15.

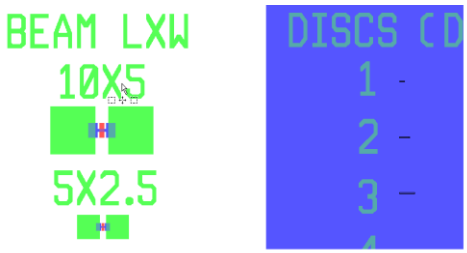

Figure 15: Snapshot of layout generated for silicon transfer chip for resonator devices

The mask has not been fabricated, because a suitable test mask was identified (having 0.8- 4 μm features), and chips already fabricated from this mask were eventually located. These chips are used in the transfer trials.

4. CONCLUSIONS

Because of its unique material properties, graphene is an ideal candidate for a resonator material. It has very high Young's modulus, is naturally one atom thick, and despite its miniscule thickness, is highly electrically conductive, and nearly impermeable to gasses and liquids.

Despite these promising properties, graphene is far from the easiest material to use in fabrication, having been first isolated only in 2004. Methods to date either mechanically exfoliate it from graphite in tiny flakes, or grow it on another substrate and then transfer it to the host substrate. This work presents novel methods for transferring CVD grown graphene.

Because of the magnitude of the intrinsic strain in known deposition methods, analysis of resonators must include both tension and bending stiffness terms in calculating resonant frequencies. Combined with a clamped (support) boundary, the analysis requires numerical methods for exact solutions. Both transcendental analytical methods and finite element methods are suitable. The value for strain in the novel CVD-transferred method is not yet known.

Planar device dimensions of L_{beam}= 1 to10 μm or r_{disc}= 1 to10 μm should provide devices with resonant frequencies in the 10-15 MHz range, within a large range of possible intrinsic strain.

5. REFERENCES

[1] http://www.wikipedia.com/Graphene

[2] Novoselov K S, Jiang D, Schedin F, Booth T J, Khotkevich V V, Morozov S V and Geim A K 2005 Two-dimensional atomic crystals *Proc. Natl Acad. Sci. USA* **102** 10451–3

[3] Timoshenko, S.; Young, D. H.; Weaver, W. *Vibration Problems in Engineering*, 4th ed.; John Wiley and Sons, Inc.: New York, 1974; pp 481-484.

[4] Bunch J S, van der Zande A M, Verbridge S S, Frank I W, Tanenbaum D M, Parpia J M, Craighead H G and McEuen P L 2007 Electromechanical resonators from graphene sheets *Science* **315** 490–3

[5] Chen, C.; Rosenblatt, S.; Bolotin, K. I.; Kalb, W.; Kim, P.; Kymissis, I.; Stormer, H. L.; Heinz, T. F.; Hone, J. *Nat. Nanotechnol.* **2009**, 1–7.

[6] Frank I W, Tanenbauma D M, van der Zande A M and McEuen P L 2007 Mechanical properties of suspended graphene sheets *J. Vac. Sci. Technol.* B **25** 2558–61

[7] Lee C, Wei X, Kysar J W and Hone J 2008 Measurement of the elastic properties and intrinsic strength of monolayer graphene *Science* **321** 385–8

[8] Bunch J S, Verbridge S S, Alden J S, van der Zande A M, Parpia J M, Craighead H G and McEuen P L 2008 Impermeable atomic membranes from graphene sheets *Nano Lett.* **8** 2458–62

[9] Wong C, Annamalai M, Wang Z and Palaniapan M, "Characterization of nanomechanical graphene drum structures" J. Micromech. Microeng. **20** (2010)

[10] Hertel, T.; Walkup, R. E.; Avouris, P. *Phys. Rev. B* **1998**, *58* (20), 13870–13873.

[11] Kreyszig E, *Advanced Engineering Mathematics*, John Wiley and Sons, Inc. New York, 2006

[12] Bunch J S, *PhD Dissertation*, Cornell University, 2008.

[13] Perozziello E, *Personal communication*.

[14] Tortonese M and Kirk M, Proc. SPIE **3009**, 53 (1997).

APPENDIX A: ANSYS CODE

```
FINISH  ! Make sure we are at BEGIN level
/CLEAR  ! Clear model since no SAVE found
/PREP7

yMod=1000
prat=0.16
dens=2.2e-24
thickness=0.335
radius=1000
elemSize=15
numModes=15


ET,1,SHELL181   ! sets element type

! Set material properties
MPTEMP,,,,,,,,
MPTEMP,1,0
MPDATA,EX,1,,yMod
MPDATA,PRXY,1,,prat
MPTEMP,,,,,,,,
MPTEMP,1,0
MPDATA,DENS,1,,dens

! Set section properties (membrane thickness)

sectype,1,shell,,
secdata, thickness,1,0.0,3
secoffset,MID

! Create geometry
CYL4,0,0,radius,0,,90
CYL4,0,0,radius,90,,180
CYL4,0,0,radius,180,,270
CYL4,0,0,radius,270,,360

aglue,all

ESIZE,elemSize,0,
MSHAPE,0,2D
MSHKEY,0

AMESH,all
```

```
FINISH
/SOL

allsel,all
lsel,u,loc,x,0
lsel,u,loc,y,0
DL,all, ,ALL,0
allsel,all

! Setup analysis
ANTYPE,2
MODOPT,LANB,numModes
EQSLV,SPAR
MXPAND,numModes, , ,0
LUMPM,0
PSTRES,0
MODOPT,LANB,numModes,0,0, ,OFF
/STATUS,SOLU

! Solve
SOLVE
FINISH
/POST1
SET,FIRST
PLNSOL, U,SUM, 0,1.0
```

DISTRIBUTION

1 Drazen Fabris
Santa Clara University
School of Engineering
Department of Mechanical Engineering
500 El Camino Real
Santa Clara, CA 95053

1 Anton Filatov
18248 W. 58th Place # 36
Golden, CO 80403
afilatov@mymail.mines.edu (electronic copy)

3 Maria Suggs
855 El Camino Real, ste 13A-126
Palo Alto, CA 9301

1	MS0892	Laura Biedermann	1748 (electronic copy)
1	MS1069	Maryam Ziaei-Moayyed	1719 (electronic copy)
1	MS1069	Mike Baker	1719 (electronic copy)
1	MS1080	Keith Ortiz	1719 (electronic copy)
1	MS1080	Paul Resnick	1719 (electronic copy)
1	MS1080	Jose Luis Cruz-Campa	1719 (electronic copy)
1	MS1084	Matt Eichenfield	1748 (electronic copy)
1	MS1084	Michael D. Henry	1746 (electronic copy)
1	MS1084	Richard Dondero	1748 (electronic copy)
1	MS0899	Technical Library	9536 (electronic copy)


Sandia National Laboratories